Theoretical description of improving measurement accuracy for incoherence Mie Doppler wind lidar*

Du Jun(杜 军), Ren De-Ming(任德明)†, Zhao Wei-Jiang(赵卫疆), Qu Yan-Chen(曲彦臣), Chen Zhen-Lei(陈振雷), and Geng Li-Jie(耿利杰)

National Key Laboratory of Tunable Laser Technology, Harbin Institute of Technology, Harbin 150001, *China*

(Received 5 June 2012; revised manuscript received 29 June 2012)

For the nonlinearity of Fabry–Perot interferometer (FPI) transmission spectrum, the measurement uncertainty of incoherent Mie Doppler wind lidar based on it increases evidently with the increase of backscattering signal Doppler shift. A method of repeating the use of the approximate linear part of FPI transmission spectra for reducing the high uncertainty of a big Doppler shift is proposed. One of the ways of realizing this method is discussed in detail, in which the characteristics of FPI transmission spectrum changing with thickness and incident angle are utilized simultaneously. Under different atmosphere conditions, it has been proved theoretically that the range of measurement uncertainty drops to one-sixth while its minimum has no serious change. This method can be used not only to guide the new system design, but also as a new working way for the fabricated system.

Keywords: incoherent Doppler wind lidar, measurement accuracy

PACS: 42.68.Wt, 42.79.Qx **DOI:** 10.1088/1674-1056/22/2/024211

1. Introduction

The wind data throughout the troposphere and stratosphere are the most important parameters[1,2] for both weather forecasting and climate studies. The lidar has been proved to be an effective apparatus to fulfill this data measurement requirement for high accuracy and spatial resolution.[3–6] The Doppler wind lidar (DWL) systems fall into two categories according to operating modes: coherent (or heterodyne[7,8]) detection system and direct detection (or incoherent[9–11]) system. There are usually two leading kinds of incoherent DWL measurement mechanisms. One is called the edged technique;[12–14] the other is the fringe-imaging technique.[15,16] For incoherent edge detection, there are two traditional methods: the single-edge of the iodine vapor filter (IVF)[10] and the double-edge technique based on the Fabry–Perot interferometer (FPI).[17] Due to the control of the free spectral range (FSR) of the FPI, usually the FPI with small FSR at long wavelength, for example 1064 nm, is used for wind measurement with Mie backscatter from the aerosol and the FPI with large FSR at short wavelength, for example 355 nm, is adopted for wind measurement with Rayleigh backscatter from molecules.[18–20]

In the incoherent Mie DWL, a double-channel FPI with different cavity spacings is used to construct the double-edge Doppler frequency discriminator for distinguishing Mie and Rayleigh scatterings to increase its sensitivity and measurement accuracy. The frequency of outgoing laser is locked at the crossing point of two transmission curves of this double-channel FPI. The backscatter signal Doppler shifted due to the atmosphere bulk movement is split between these two channels. Their transmittances through the FPI vary with the magnitude of the Doppler shift. The differential measurements of the transmittances of outgoing laser and atmospheric backscatter signal can be made to retrieve the Doppler shift, which can be used to determine the wind velocity in the line-of-sight of the outgoing laser direction. With the structure parameters given in Ref. [9], and the atmosphere temperature $T = 273$ K, the transmission spectra for Mie and Rayleigh backscatters can be calculated (with Eqs. (8) and (9) in Section 2) as shown in Fig. 1(a). From Fig. 1(a) it can be found that the measuring dynamic range of this FPI is about ± 110 MHz relative to the outgoing laser frequency (which is assumed to be 0 MHz), corresponding to about ± 50 m/s wind velocity in the line-of-sight of the outgoing laser direction. Though the double-edge FPI Mie DWL is Rayleigh-corrected method, the Rayleigh component can be removed from the transmission signal through these two channels, the shot noise of Rayleigh backscatter still exists and affects the measuring accuracy. Under the assumption of the ratio of Mie backscattering cross section to the Rayleigh backscattering cross section $R_a = 2$ and total received photon number $N_0 = 5000$, the measuring uncertainty for a signal shot-noise-limited case is shown in Fig. 1(b). It can be found that the measuring uncertainty (2.78 m/s∼9.76 m/s) is not the same for different Doppler frequency shifts, its minimum is at the zero Doppler shift and its value increases with Doppler frequency increasing. For an outstanding measuring instrument, the measuring uncertainty should be low in the whole measuring dynamic range no matter what the measuring

*Project supported by the International Cooperative Project between China and Russia, Research on the Ocean/Atmosphere Lidar (Grant No. 2008DFR10170).
†Corresponding author. E-mail: deming@hit.edu.cn
© 2013 Chinese Physical Society and IOP Publishing Ltd

value is. So the present method of wind measurement contains defects.

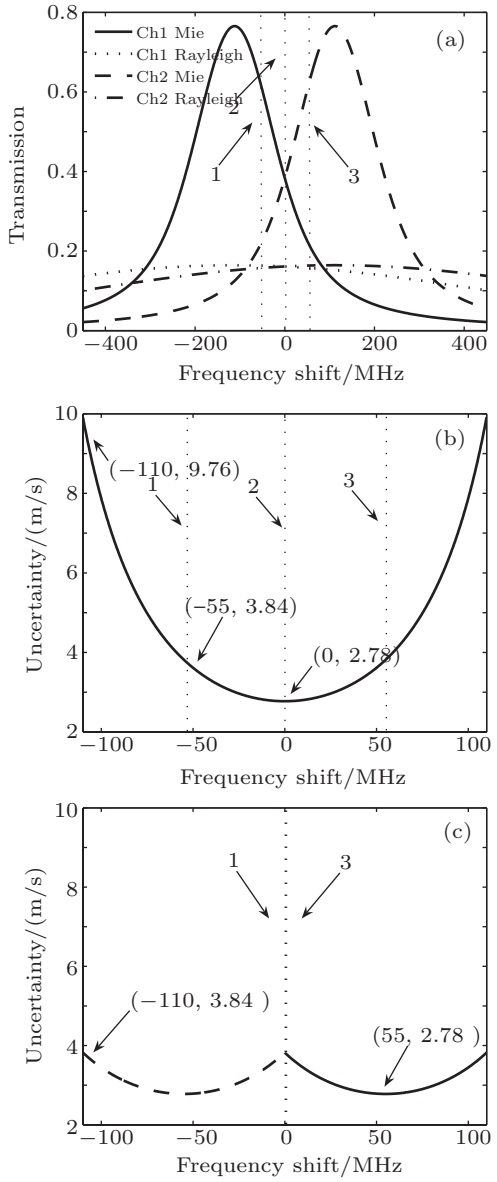


Fig. 1. (a) Transmission spectra of the double-edge FPI system, (b) the uncertainty of the double-edge FPI system, (c) the uncertainty of the double-edge FPI system for direction distinguishing measurement.

There are two main factors that affect the measuring accuracy, that is, the measuring sensitivity and signal-to-noise ratio (SNR) (see Eq. (11) in Section 2). For the nonlinearity of the FPI transmission curves,[21,22] both of them decrease with Doppler shift of atmosphere backscatter signal increasing (see Figs. 4(a) and 4(b) in Subsection 3.2), which leads to the increase of uncertainty. So, the measuring accuracy requirement can be easily fulfilled for lower wind velocity, but not for higher wind velocity. If we could only utilize the approximate linear part of transmission curves with high sensitivity and SNR for any wind velocity measurement, the uncertainty would always be low. For the excellent transmission curve part (the approximate linear parts 1 to 3 in Fig. 1(a)) that does not fulfill the measuring dynamic range requirement (± 50 m/s wind velocity in the line-of-sight of outgoing laser direction), we propose to repeat the use of it. With the parameter of FPI and backscattering light unchanged, we can make the frequency of the outgoing laser be at location 3 or location 1 in Fig. 1(a) alternately. With location 1, the wind velocity against the line-of-sight of outgoing laser within 0 m/s$\sim$50 m/s can be measured with transmission curve from locations 1 to 3 in Fig. 1(a), and the uncertainty for this wind velocity range is that for the part from 1 to 3 in Fig. 1(b) and shown in Fig. 1(c) with solid line when the frequency of the outgoing laser is assumed to be zero Doppler shift. With location 3, the wind toward the line-of-sight of outgoing laser within 0 m/s $\sim$ 50 m/s can be measured with transmission curve from 3 to 1, and the uncertainty for this wind velocity range is that for the part from 3 to 1 in Fig. 1(b) and shown in Fig. 1(c) with dashed line too. Following this way, the whole measuring uncertainties are all in a range between 2.78 m/s and 3.84 m/s for the wind velocities along different directions within 50 m/s, i.e., the uncertainty is relatively smooth and low for different frequency shifts, except only for a small Doppler shift as shown in Fig. 1(b). Also, the error range decreases to about 1/6 compared with the previous result on the same atmosphere condition.

For the already fabricated DWL system, there will be two optional methods of tuning the location of the outgoing laser with respect to the transmission spectra of these two channels. One is that the cavity spaces of the double-edge FPI system are changed by the piezoelectric ceramics to move the whole transmission spectra with the frequency of outgoing laser kept unchanged, and the other is that the frequency of the outgoing laser is shifted with an acousto-optic frequency shifter[23] with the transmission curves of the FPI system kept unchanged.

The method provided above not only can be utilized as a new way of working for the existing system, but also can be used to design a new DWL system. The purpose of this paper is to introduce a workable method for this kind of measuring, which will be easier to realize in practice.

2. Theory

Assume the surface defect of the FPI follows the Gaussian probability distribution, then the transmission function of FPI can be shown as follows:[24]

$$h_1 = C\left\{1+2\sum_{n=1}^{\infty} R^n \cos(n\varphi)\exp\left[-\frac{1}{4}n^2\varphi^2\left(\frac{\Delta d_{\mathrm{D}}}{d_0}\right)^2\right]\right\}. \quad (1)$$

In Eq. (1),

$$C = \left(1-\frac{\mathrm{A}}{1-R}\right)^2\left(\frac{1-R}{1+R}\right), \quad (2)$$

$$\varphi = \frac{4\pi\mu d_0 \nu_0 \cos\theta_0}{c}, \quad (3)$$

where μ is the refractive index between the FPI plates, d_0 is the plate separation, ν_0 is the frequency of the incident light, θ_0 is the incident angle of light between plates, A denotes any scattering and absorptive losses in the FPI plates, R is the plate reflectivity, c is the light velocity in air, and Δd_{D} denotes the FPI surface defect.

The FPI is usually illuminated by light collimated with an angular field of view θ_{M} (semi-angle). Therefore, the transmission function can be written as

$$h_2 = \frac{1}{\pi\theta_{\mathrm{M}}^2}\int_{-\theta_{\mathrm{M}}}^{\theta_{\mathrm{M}}} A(\theta_0,\theta)\sin(\theta_0+\theta)\,h_1(\nu_0,\theta_0+\theta)\,\mathrm{d}\theta, \quad (4)$$

where

$$A(\theta_0,\theta) = \begin{cases} 0, & 0\le\theta_0\le\theta_{\mathrm{M}},\ \theta_0-\theta_{\mathrm{M}}\le\theta_0+\theta\le 0, \\ 2\pi, & 0\le\theta_0\le\theta_{\mathrm{M}},\ 0<\theta_0+\theta\le\theta_{\mathrm{M}}-\theta_0, \\ 2\mathrm{arc}\left(\dfrac{\cos\theta_{\mathrm{M}}-\cos(\theta_0+\theta)\cos\theta_0}{\sin\theta_0\sin(\theta_0+\theta)}\right). \end{cases} \quad (5)$$

Both the aerosol and molecule backscatter spectra, $f_{\mathrm{M}}(\nu)$ and $f_{\mathrm{R}}(\nu)$, have Gaussian profiles. They can be given by[9]

$$f_{\mathrm{M}}(\nu) = \left(4\ln 2/\pi\Delta\nu_{\mathrm{M}}^2\right)^{1/2}\exp\left(-\nu^2 4\ln 2/\Delta\nu_{\mathrm{M}}^2\right), \quad (6)$$

$$f_{\mathrm{R}}(\nu) = \left(4\ln 2/\pi\Delta\nu_{\mathrm{R}}^2\right)^{1/2}\exp\left(-\nu^2 4\ln 2/\Delta\nu_{\mathrm{R}}^2\right), \quad (7)$$

where $\Delta\nu_{\mathrm{M}}$ is the line width of the Mie backscatter spectrum from the atmosphere. Because the Brownian motion of the aerosol particle does not broaden the spectrum significantly, it can be replaced by the line width of the outgoing laser. Hence, in this paper, the Mie backscatter spectrum $f_{\mathrm{M}}(\nu)$ is replaced by the outgoing laser spectrum $f_{\mathrm{L}}(\nu)$. The line width of the atmospheric Rayleigh spectrum is $\Delta\nu_{\mathrm{R}} = \left(32kT\ln 2/\lambda^2 M\right)^{1/2}$, where k is the Boltzmann constant, T is the atmosphere temperature, M is the averaging mass of the atmospheric molecules, and λ is the laser wavelength.

The transmission function for Mie backscatter is written as a convolution function

$$\begin{aligned} T_{\mathrm{M}} &= \int_{-\infty}^{\infty} h_2(\nu_0-\nu')\,f_{\mathrm{M}}(\nu')\,\mathrm{d}\nu' \\ &= \int_{-\infty}^{\infty} h_2(\nu_0-\nu')\,f_{\mathrm{L}}(\nu')\,\mathrm{d}\nu'. \end{aligned} \quad (8)$$

The transmission function for Rayleigh backscatter is a convolution of the transmission function (Eq. (4)), laser spectrum, and the Rayleigh spectrum. It can be given by

$$T_{\mathrm{R}} = \int_{-\infty}^{\infty} T_{\mathrm{M}}(\nu_0-\nu')\,f_{\mathrm{R}}(\nu')\,\mathrm{d}\nu'. \quad (9)$$

The ratio (response) of transmittances between these two measuring channels is used as the measuring metric to retrieve the Doppler shift and is shown as

$$R(\nu) = \frac{T_{\mathrm{M1}}(\nu)}{T_{\mathrm{M2}}(\nu)}, \quad (10)$$

where $T_{\mathrm{M1}}(\nu)$ and $T_{\mathrm{M2}}(\nu)$ are the transmittances of two channels for the outgoing laser and Mie backscatter signal.

The measuring uncertainty in the line-of-sight wind velocity is given as[14]

$$\varepsilon = \frac{1}{(S/N)\,\Theta}, \quad (11)$$

where S/N is the signal-to-noise ratio (SNR) for the double-channel measurement of Eq. (10). The sensitivity Θ of the double-channel measurement is the fractional change in the transmittance ratio of Eq. (10) for a unit wind velocity in the line-of-sight of outgoing laser.

3. Design for improving measurement accuracy

3.1. Structure and principle

As is well known, the transmission curve of FPI moves not only with the interval of its plates, but also with the incident angle of light. So Kim *et al.*[25] proposed the single etalon double-edge DWL receiving optical system, and they inputted two signal lights with different incident angles on an FPI, the transmission spectra of which would part from each other and a different double-edge system is realized. We can name this the angle-double-edge FPI system, and the previous one (two beams with the same incident angle into the double-channel FPI with different intervals) is named thickness-double-edge FPI system for distinguishing them in this paper. Shift these two incident signal lights to fall on other FPIs with different cavity spaces, then their whole transmission spectra will move with their patterns kept unchanged. In this way, we can use the approximate linear part of transmission curves of these two angle-double-edge FPI structures, alternately, for measuring the wind velocities in different directions. The schematic diagram of this method is shown in Fig. 2.

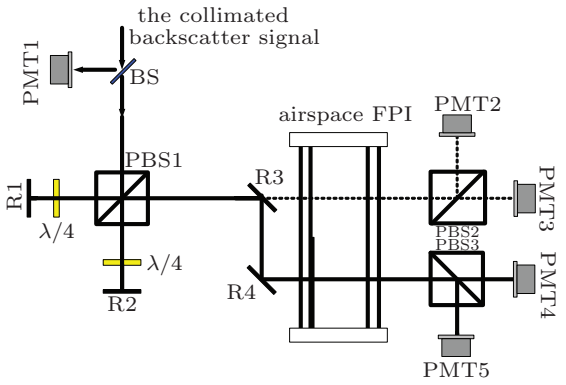


Fig. 2. (color online) Schematic diagram for the angle-double-edge FPI structure for direction distinguishing wind measurement.

The backscatter of the atmosphere after collimation, is split into two beams by beam splitter BS, about 20% is inputted into the energy monitor (Photomultiplier PMT1); the 80% is inputted into the polarization beam splitter (PBS1) and split into two beams with different polarizations towards the

FPI. By rotating the reflectors R1 and R2, the incident angles of these two beams can be tuned. Let one incident angle be $\theta_1 = 0$ mrad, the other angle be $\theta_2 = 1.25$ mrad. When the reflector R3 is removed, these two beams pass through the upper half of the FPI with bigger cavity space, and PBS2 divides these two signal light beams toward the signal monitors PMT2 and PMT3. The normalized FPI transmission signal for these two signals can be obtained by taking a ratio between the signal PMT2 and PMT3 with the energy monitor signal PMT1. Using the parameters of FPI that are the same as those given by Xia *et al*.[9] and the atmosphere temperature $T = 273$ K, the laser line width and half divergence angle are $\nu_L = 60$ MHz, $\theta_M = 60$ mrad respectively, the transmission spectra of these two beams for aerosol and molecule backscatter are calculated and shown in Fig. 3(a). An angle-double-edge FPI system can be realized in this way. The measuring uncertainty of this structure is calculated and shown in Fig. 3(b) under the assumption of Mie and Rayleigh backscatter ratio $R_a = 2$ and total received photon number $N_0 = 5000$ too. We can make a horizontal line cross the uncertainty curve at two points (−72, 4.02) and (38, 4.02), and the frequency interval of these two points is about 110 MHz. These two locations are marked with 1 and 3 in Fig. 3(b) (and the corresponding marked points in Fig.3(a)). We can lock the frequency of outgoing laser at location 3 by thickness tuning the airspace FPI. Then we put the R3 at the location in Fig. 2. These two beams pass through the lower part of the FPI which has a narrower cavity space, and are divided into two signal monitors PMT4 and PMT5. The thickness difference between these two parts of the FPI is about 17 nm corresponding to 110-MHz Doppler shift. The transmission spectra and measuring uncertainties of these two beams in the lower part of the FPI are calculated too, which have the same patterns as shown in Fig. 3(a) and Fig. 3(b), except for location 1 of outgoing laser. So following this way (removing and putting back R3) to shift the location of outgoing laser, we can easily alternately use the excellent transmission curves (from 1 to 3 in Fig. 3(a)) of these two angle-double-edge FPI structures to measure the wind velocity against or along the line-of-sight of outgoing laser direction. The measuring uncertainty is shown in Fig. 3(c). The error range is from 2.79 m/s to 4.0 2m/s and is about 1/6 of the previous error range (Fig. 1(b)).

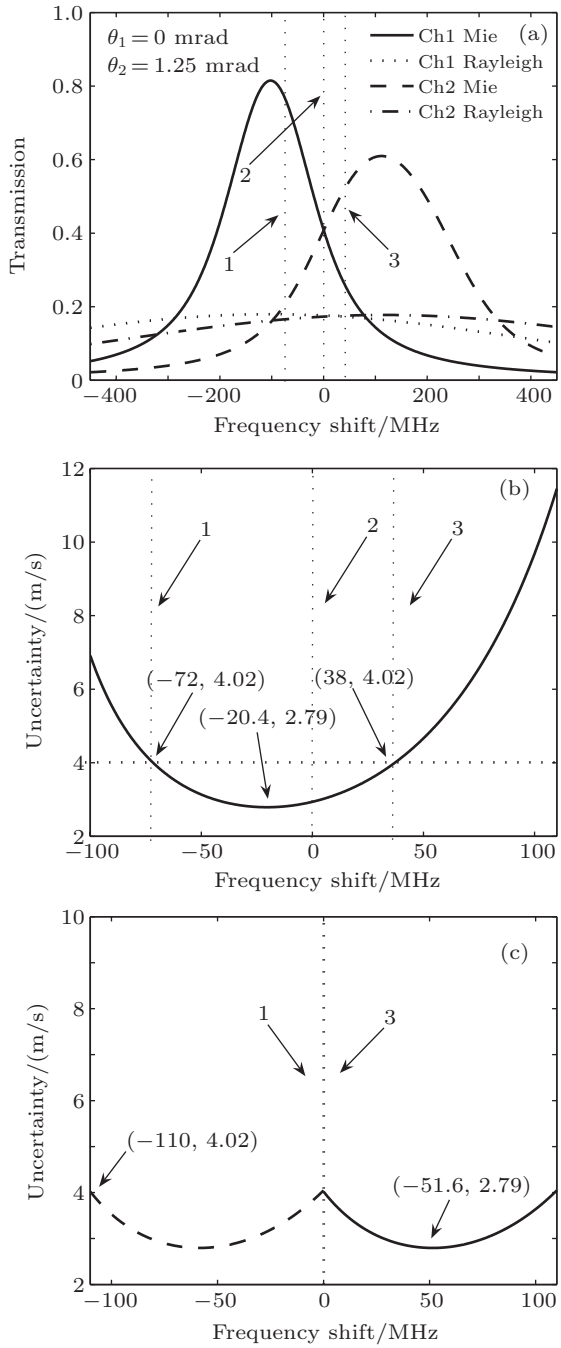


Fig. 3. (a) Transmission spectra of the angle-double-channel FPI, (b) the uncertainty of the angle-double-channel FPI, and (c) the uncertainty of the angle-double-channel FPI for direction distinguishing measurement.

3.2. Discussion about the angle-double-edge FPI system

In Fig. 3(a), it can be found that the peak transmission of non-normal incident light is lower than that of the normal incident light,[25] so the measuring sensitivity and SNR of the angle-double-edge structure will be asymmetric and lower than those of the thickness-double-edge structure with same structure parameters. To obtain the same measuring accuracy, some changes are made for the angle-double-edge FPI system. The half divergent angle of the incident light is reduced from 0.5 mrad to 0.4 mrad which will require a bigger diameter of the FPI, and the laser line width is reduced from 90 MHz to 60 MHz. On this condition, the peak transmissions of angle-double-edge structure become higher to make up for

the decrease of measuring accuracy caused by the asymmetries of transmission curves. With the same structure parameters, except for divergence angle and laser line width, the measuring sensitivity and SNR of these two structures are shown and compared in Figs. 4(b) and 4(c).

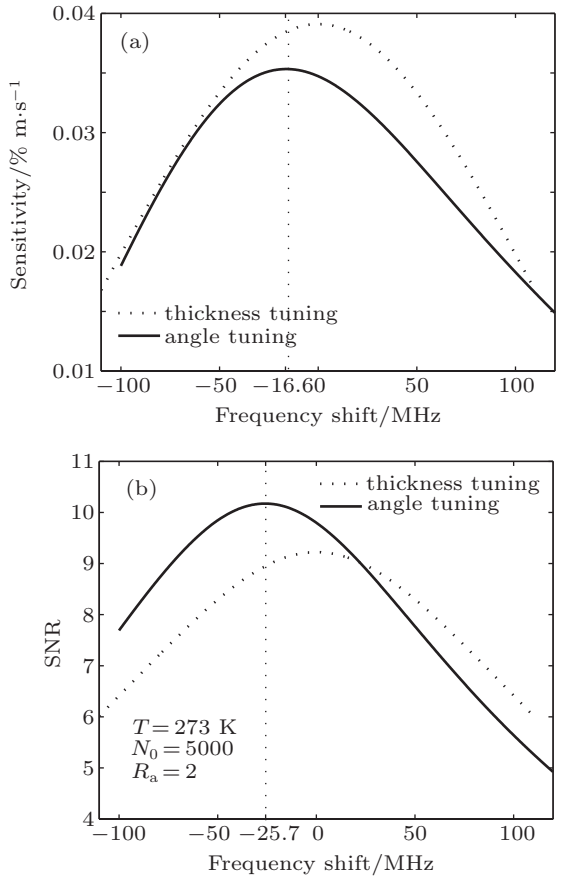


Fig. 4. (a) Sensitivity for the angle-double-channel FPI structure, (b) SNR for the angle-double-channel FPI structure.

As shown in Figs. 4(a) and 4(b), the measured dynamic ranges of these two structures are the same (220 MHz). However, the measured dynamic range for angle-double-edge is asymmetric (−100 MHz∼120 MHz), while that for the thickness-double-edge is symmetric (−100 MHz∼110 MHz). Nearly, the whole measuring sensitivity of the angle-double-edge is lower than that of the thickness-double-edge, and the maximum sensitivity of the angle-double-edge structure is not at the zero Doppler shift location as shown in Fig. 4(a). The SNR of the angle-double-edge is higher than that of the thickness-double-channel in the half measurement dynamic range and the maximum is not at the zero Doppler shift location either under the atmosphere condition mentioned in Subsection 3.1. Because the measured uncertainty is related to the measurements of sensitivity and SNR, the minimum values of uncertainty for these two structures are almost the same and the error curve of angle-double-edge is not superposed on that of the thickness-double-edge as shown in Figs. 1(b) and 3(b). Obviously, utilizing the whole transmission curve of the angle-double-edge to measure the whole wind velocity will have certain defects for the asymmetric transmission spectra. But for partly using the transmission curve of the angle-double-edge, the defect of this structure is not so evident as the above discussion.

3.3. Simulation of the measurement accuracy under different atmosphere parameters

The measuring uncertainty is related to the received photon, the Mie and Rayleigh scattering ratio, and the temperature of atmosphere. Figure 5 shows a comparison of the measurement uncertainty between the normal thickness-double-edge and the angle-double-edge for direction distinguishing measurement under different atmosphere conditions.

The results show that with the atmosphere condition varying, all the measured uncertainties obtained from these two methods are changed. With the decreases of received photon N_0, Mie and Rayleigh backscatter ratio R_a and temperature of atmosphere T, all the measured uncertainties and the uncertainty range increase. By using this measuring method provided above, the range of measured uncertainty decreases to about $1/6$ under different conditions when the minimum uncertainty is the same as that of the thickness-double-edge. So this method will be effective for different atmosphere conditions.

As shown in Fig. 5, though the measured uncertainty under big Doppler frequency by using the method provided above is evidently lower than that of the thickness-double-edge, the measured uncertainty near its zero Doppler frequency shift is slightly higher than that of the thickness-double-edge. We can use the previous way (outgoing laser locked at the minimum measurement uncertainty point) to roughly measure the atmosphere wind. If the whole Doppler shift due to wind movement in the line-of-sight is in a range of about ±30 MHz (about ±17 m/s), there is no need to use this way because in this Doppler shift range the measurement accuracy of the previous way is already high. If there is Doppler shift beyond this range at a certain height, re-measurement at this height with the new way should be made for high measurement accuracy. The above method can also provide a supplement for the existing Mie DWL system which is based on the thickness-double-edge or angle-double-edge FPI system.

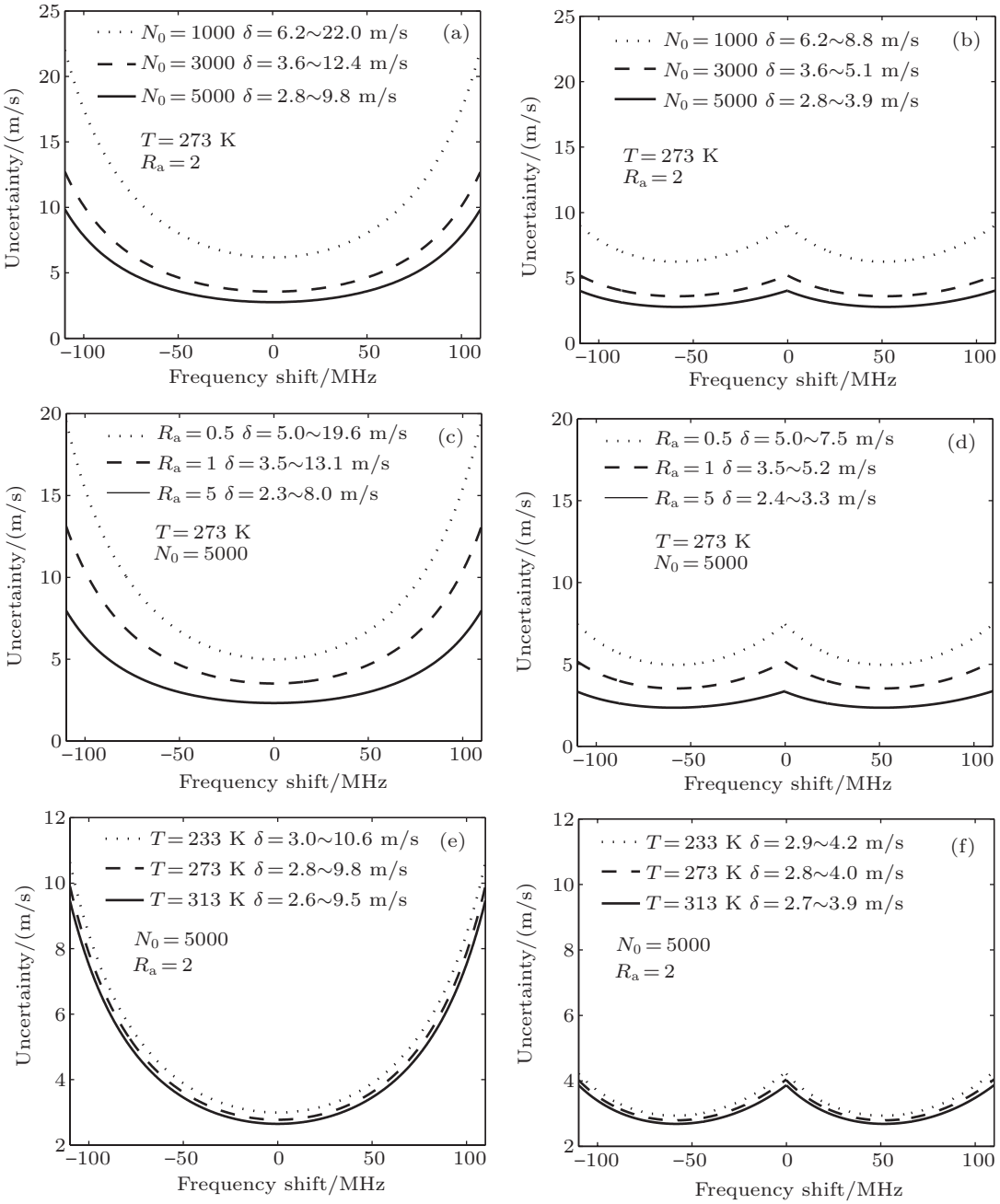


Fig. 5. (a) and (b): Uncertainties of thickness-double-channel and direction distinguishing angle-double-channel under different values of received photon number N_0, (c) and (d) uncertainties of these two methods under different values of Mie and Rayleigh ratio R_a, (e) and (f) uncertainties of these two methods under different values of temperature T.

4. Conclusion

Because both the measuring sensitivity and SNR of double-channel FPI structure in Mie DWL system decrease with Doppler shift increasing, the measurement error increases evidently. This will not make the DWL fulfill the measuring requirements under bigger wind velocity in the line-of-sight of outgoing laser. For this reason, the repeated use of the excellent part of the transmission curve with relatively high sensitivity and SNR to measure the wind velocities of different directions in the line-of-sight of outgoing laser is suggested. The different methods of realizing this manner are provided and alternately using the transmission curves of two angle-double-edge FPI systems with different cavity spaces is discussed in detail. After simulating this structure, it is proved that this structure can reduce the measurement error range to $1/6$ of the range for the previous structure, while the minimum uncertainty is unchanged under different measurement conditions. This method to increase the measurement accuracy can serve as a supplement to the normal DWL or a principle for designing a new system.

References

[1] Zhao P T, Zhang Y C, Wang L, Hu S X, Su J, Cao K F, Zhao Y F and Hu H L 2008 *Chin. Phys.* B **17** 335

[2] Zhao P T, Zhang Y C, Wang L, Zhao Y F, Su J, Fang X, Cao K F, Xie J and Du X Y 2007 *Chin. Phys.* **16** 2486

[3] Zhang C M, Ai J J and Ren W Y 2011 *Chin. Phys.* B **20** 020701

[4] Zhong J, Huang S X, Fei J F, Du H D and Zhang L 2011 *Chin. Phys.* B **20** 064301

[5] Zhong J, Huang S X, Du H D and Zhang L 2011 *Chin. Phys.* B **20** 034301

[6] Mu T K and Zhang C M 2010 *Chin. Phys.* B **19** 060702

[7] Bai Y, Zhao W J, Ren D M, Qu Y C, Liu C, Yuan J H, Qian L M and Chen Z L 2012 *Acta Phys. Sin.* **61** 094218 (in Chinese)

[8] Li Y C, Zhang L, Yang Y L, Gao L, Xu B and Wang C H 2009 *Acta Phys. Sin.* **58** 5473 (in Chinese)

[9] Xia H Y, Sun D S, Yang Y H, Shen F H, Dong J J and Kobayashi T 2007 *Appl. Opt.* **46** 7120

[10] Liu Z S, Liu B Y, Wu S H, Li Z G and Wang Z J 2008 *Opt. Lett.* **33** 1485

[11] Foster M J, Bond R, Storey J, Thwaite C, Labandibar J Y, Bakalski I, Hélière A, Delev A, Rees D and Slimm M 2009 *Opt. Express* **17** 3476

[12] Souprayen C, Garnier A and Hertzog A 1999 *Appl. Opt.* **38** 2422

[13] Korb C L, Gentry B M, Li S X and Flesia C 1998 *Appl. Opt.* **37** 3097

[14] Flesia C and Korb C L 1999 *Appl. Opt.* **38** 432

[15] McGill M J, Skinner W R and Irgang T D 1997 *Appl. Opt.* **36** 1253

[16] Belmonte A and Lázaro A 2006 *Opt. Express* **14** 7699

[17] Gentry B M, Chen H L and Li S X 2000 *Opt. Lett.* **25** 1231

[18] Mckay J A 1999 *Appl. Opt.* **38** 5859

[19] Tang L, Shu Z F, Dong J H, Wang G C, Wang Y T, Xu W J, Hu D D, Chen T D, Dou X K, Sun D S and Cha H 2010 *Chin. Opt. Lett.* **8** 726

[20] Dong J H, Cha H, Kim D, Baik S H, Wang G C, Tang L, Shu Z F, Xu W J, Hu D D and Sun D S 2010 *J. Opt. Soc. Korea* **14** 199

[21] Li Y C and Wang C H 2012 *Chin. Phys.* B **21** 020701

[22] Li Y C, Wang C H, Qu Y, Gao L, Cong H F, Yang Y L, Gao J and Wang A Y 2011 *Chin. Phys.* B **20** 014208

[23] Mckay J A 1998 *Appl. Opt.* **37** 6480

[24] She C Y and Yu J R 1994 *Geophys. Res. Lett.* **21** 1771

[25] Kim D, Kwon S, Cha H, Kim Y and Sunwoo J 2008 *Rev. Sci. Instrum.* **79** 123111